Synthesis and characterization of bistropolonato oxovanadium(IV and V) complexes

Beatriz S. Parajón-Costa[a]; Enrique J. Baran[a]; Julio Romero[b]; Regino Sáez-Puche[b]; Gabriel Arrambide[c]; Dinorah Gambino[c]

[a] Centro de Química Inorgánica (CEQUINOR/CONICET,UNLP), Facultad de Ciencias Exactas, Universidad Nacional de La Plata, 1900-La Plata, Argentina [b] Departamento de Química Inorgánica, Facultad de Ciencias Químicas, Universidad Complutense de Madrid, E-28040 Madrid, Spain [c] Departamento "Estrella Campos", Cátedra de Química Inorgánica, Facultad de Química, Universidad de la República, Montevideo, Uruguay

PLEASE SCROLL DOWN FOR ARTICLE

Taylor & Francis
Taylor & Francis Group

Synthesis and characterization of bistropolonato oxovanadium(IV and V) complexes

BEATRIZ S. PARAJÓN-COSTA†, ENRIQUE J. BARAN*†, JULIO ROMERO‡,
REGINO SÁEZ-PUCHE‡, GABRIEL ARRAMBIDE§ and DINORAH GAMBINO§

†Centro de Química Inorgánica (CEQUINOR/CONICET,UNLP), Facultad de Ciencias
Exactas, Universidad Nacional de La Plata, C. Correo 962, 1900-La Plata, Argentina
‡Departamento de Química Inorgánica, Facultad de Ciencias Químicas, Universidad
Complutense de Madrid, E-28040 Madrid, Spain
§Departamento ''Estrella Campos'', Cátedra de Química Inorgánica, Facultad de Química,
Universidad de la República, Montevideo, Uruguay

Oxovanadium(IV) and oxovanadium(V) complexes of tropolone (Htrp, 2-hydroxy-2,4,6-cycloheptatrien-1-one), of stoichiometry $VO(trp)_2$ and $VO(trp)_2Cl$, were characterized by electronic, infrared, and Raman spectroscopies. Their electrochemical behavior was investigated by cyclic voltamperommetry in dimethylsulfoxide solutions. The magnetic susceptibility of $VO(trp)_2$ was investigated between 2 and 300 K. The vibrational spectra of the related $Co(trp)_2$, $Cu(trp)_2$, and $Zn(trp)_2$ complexes were also analyzed for comparative purposes.

Keywords: Tropolone; Oxovanadium complexes; Electronic spectra; IR and Raman spectra;
Cyclic voltamperommetry; Magnetic susceptibility

1. Introduction

A number of metal complexes of hydroxypyrones and hydroxypyridinones have been prepared and characterized and their possible applications in the field of medicinal inorganic chemistry have been explored [1]. Most of these α-hydroxyketones, derived from six-membered rings, form relatively stable complexes with different divalent and trivalent cations. In particular, oxovanadium(IV) complexes of 3,4-hydroxypyrones, such as bis(maltolato)oxovanadium(IV), and other maltol derivatives, have been widely explored as insulin-enhancing agents [1–3].

Tropolone (2-hydroxy-2,4,6-cycloheptatrien-1-one, Htrp, figure 1) is a very interesting α-hydroxyketone, but derived from a seven-membered ring, which also forms stable complexes with numerous metals [4–6]. On the other hand, tropolone itself has antibacterial and insecticidal activity [7, 8], also acts as an inhibitor of metalloproteins [9], and is a strong tyrosinase inhibitor [10, 11]. Some derivatives of tropolone have antitumoral activity [12, 13], whereas some others, like β-thujaplicinol and manicol, are

---

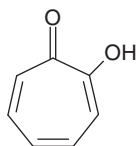*Corresponding author. Email: baran@quimica.unlp.edu.ar

Figure 1. Schematic structure of tropolone (Htrp).

potent and selective inhibitors of ribonuclease H (RNase H) activity of human immunodeficiency virus-type 1 reverse transcriptase (HIV-1RT) [14].

The crystal and molecular structure of tropolone [15] and some of its derivatives [16, 17] as well as those of the bis(tropolonato) complexes of Cu(II) [18] and Zn(II) [19] are known.

Extending previous studies on oxovanadium(IV) and oxovanadium(V) complexes [20–25] we have now investigated the complexes of these two oxocations with tropolone. The respective complexes of Co(II), Cu(II), and Zn(II) were also prepared for comparative purposes.

2. Experimental

2.1. *Materials*

Tropolone, $NaVO_3$, and $VOCl_3$ were purchased from Aldrich, $VOSO_4 \cdot 5H_2O$ and the acetates of Co(II), Cu(II), and Zn(II) as well as all the employed solvents were products of Merck, and were used as supplied. For the electrochemical measurements high purity dimethylsulfoxide (DMSO) from Aldrich was used and tetrabutylammonium hexafluorophosphate ($TBAPF_6$) from Fluka (electrochemical grade) was employed as the supporting electrolyte.

2.2. *Synthesis of the complexes*

VO(trp)$_2$ was obtained following the procedure described by Lee and Hwang [26], as follows: 0.50 g (4 mmol) of tropolone was dissolved in 100 mL of a 50 : 50 mixture of ethanol/water and added dropwise to a well-stirred solution containing 0.51 g (2 mmol) of $VOSO_4 \cdot 5H_2O$ in 50 mL of the same solvent mixture. After mixing, the pH was raised to 8.5 by the addition of 1 N NaOH and the resulting solution was refluxed with stirring for 2 h and then left at room temperature. The dark green powder was filtered off, washed with small portions of cold ethanol, and finally dried in vacuum over H_2SO_4. Analysis: Found (%): C: 54.33, H: 3.30 (calculated for VO(trp)$_2$ (%): C: 54.38, H: 3.23).

VO(trp)$_2$Cl was prepared by the addition of 10 mmol of $VOCl_3$ to a solution of 40 mmol of tropolone in 100 mL of CCl_4. The reaction occurs immediately, but the reaction mixture was stirred overnight to ensure completion [27]. The dark black-green product was filtered off, washed repeatedly with CCl_4, and finally dried in vacuum over H_2SO_4. Analysis: Found (%): C: 48.20, H: 3.05 (calculated for VO(trp)$_2$Cl (%): C: 48.78, H: 2.90). The suggested use of triethylamine, to facilitate the formation of

tropolonate in solution [27], was avoided because the so generated complexes usually remain contaminated with the base, as shown by infrared (IR) spectra.

We have also developed an alternative procedure for the synthesis of VO(trp)$_2$Cl, based on a known analytical methodology [28], as follows: 0.52 g (4.3 mmol) of NaVO$_3$ was dissolved in 20 mL of distilled water and 5 mL of concentrated HCl was added. Eventually precipitated V$_2$O$_5$ was filtered off. Then, 1.10 g (9 mmol) of tropolone was dissolved in 20 mL of CH$_3$Cl and this solution was added dropwise to that containing the vanadium under continuous stirring. The mixture is stirred for one more hour and then the obtained VO(trp)$_2$Cl was separated by filtration, washed with several portions of CCl$_4$, and finally dried in vacuum over H$_2$SO$_4$. Analytical data and FTIR spectra confirmed the identity of the obtained complex.

The complexes Co(trp)$_2$, Cu(trp)$_2$, and Zn(trp)$_2$ were obtained by slow mixing 50 : 50 methanol : water solutions of tropolone and the metal acetates in a 2 : 1 molar ratio and refluxing the obtained mixtures, with stirring, for 2 h [6, 18]. The obtained crystals were separated by filtration, washed several times with cold methanol, and finally dried in vacuum over H$_2$SO$_4$.

2.3. Spectroscopic measurements

IR spectra in the spectral range between 4000 and 400 cm^{-1} were measured as KBr pellets on a FTIR-Bruker-EQUINOX-55 instrument. Raman spectra were recorded with the FRA 106 accessory of a Bruker IF 66 FTIR spectrophotometer. The 1064 nm line of an Nd : YAG solid state laser was used for excitation.

Electronic absorption spectra were measured in the 200–800 nm spectral range with a Hewlett-Packard 8452 diode-array spectrophotometer using 10 mm quartz cells.

2.4. Magnetic susceptibility measurements

Magnetic susceptibility measurements were performed on polycrystalline samples of VO(trp)$_2$ using a SQUID magnetometer (Quantum Design, model MPMS-XL). The temperature dependence of the magnetic susceptibility was measured in the temperature range 2–300 K at an applied magnetic field (H) of 0.5 T upon heating the sample under zero-field-cooled conditions from 2 K (previously cooled at $H = 0$ T). The paramagnetic contribution χ_P to the experimental susceptibility was obtained on subtracting the diamagnetic contribution ($-102(1) \times 10^{-6}$ emu mol^{-1}) which was calculated from Pascal's constants [29].

2.5. Electrochemical measurements

Cyclic voltammetry was carried out with a computer-controlled Princeton Applied Research (PAR) Potentiostat/Galvanostat model 263A. A standard three-electrode cell was used with a glassy carbon disc as the working electrode, a platinum wire as the counter electrode, and Ag/10^{-2} mol L^{-1} AgNO$_3$ in CH$_3$CN as the reference electrode. This electrode was calibrated against the [Fe(C$_5$H$_5$)$_2$]/[Fe(C$_5$H$_5$)$_2$]$^+$ redox couple, for which a potential of +0.4 V *versus* NHE was assumed [30, 31]. All potentials reported here are referred to NHE in volts. Measurements were performed in oxygen-purged

10^{-3} mol L^{-1} DMSO solutions with 0.1 mol L^{-1} TBAPF$_6$ as the supporting electrolyte. During the measurements a continuous N$_2$ gas stream was passed over the solutions.

3. Results and discussion

3.1. *Structural considerations*

Although the crystal structures of the two investigated oxovanadium complexes are not known, the spectroscopic information and all the other physicochemical properties determined in this study clearly show the generation of two five-membered chelate rings around the metal centers similar to those found for Cu(trp)$_2$ [18]. Both complexes are isolated as non-polymeric units with an oxo-ligand located perpendicular to the approximately planar VO$_4$ environment generated by binding two tropolonate ligands. In the case of the V(V) complex a chloride is coordinated *trans* to the oxo group. For VO(trp)$_2$, the local symmetry of the complex may be C$_{4v}$. It has been shown on the basis of EPR studies, for this and other related oxovanadium(IV) complexes with bidentate chelating ligands, that the symmetry is actually reduced to C$_{2v}$ [32].

3.2. *Electronic spectra and solution behavior of VO(trp)$_2$*

The solutions of different five-membered ring chelate complexes like VO(trp)$_2$ are relatively unstable in the presence of oxygen, especially when water or ethanol is solvent [32]. The originally green-colored solutions become rapidly orange-red on contact with air, by the oxidation of V(IV) to V(V):

$$2VO(trp)_2 + 2ROH + \tfrac{1}{2}O_2 \rightarrow 2VO(trp)_2OR + H_2O.$$
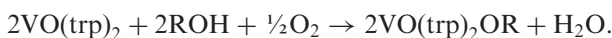
We have investigated qualitatively this behavior in different organic solvents (methanol, DMF, chloroform, THF, DMSO) and found relatively rapid color changes, from green to orange-red, in all of them. This makes it difficult to attain electronic absorption spectra with VO(trp)$_2$ solutions. In all cases, using different solvents the spectra of this complex were identical to those obtained with analogous VO(trp)$_2$Cl solutions, confirming relatively rapid oxidation of the oxovanadium(IV) solutions.

Figure 2 shows electronic spectra, in the spectral range between 260 and 500 nm, obtained with DMSO solutions of free tropolone and the two oxovanadium complexes. Measured band positions are presented in table 1. In all cases, another absorption band was detected at 260 nm (with the following ε-values: tropolone $= 4.76 \times 10^3$, VO(trp)$_2 = 20.82 \times 10^4$, and VO(trp)$_2$Cl $= 20.47 \times 10^4$). As these bands lie near the cut off edge of the solvent they have to be carefully considered. No other bands could be found, even working with more concentrated solutions. These results show clearly that independent of the origin of the dissolved complexes the obtained spectra are practically coincident, showing only minor intensity differences.

The main observed electronic transitions are $\pi\pi^*$ transitions of the aromatic ring [33] and the shoulders observed at the lower energy side in all the spectra are probably related to the characteristic vibronic structure of some of these transitions [34]. Intensity differences between the spectra of free tropolone and the complexes can be essentially
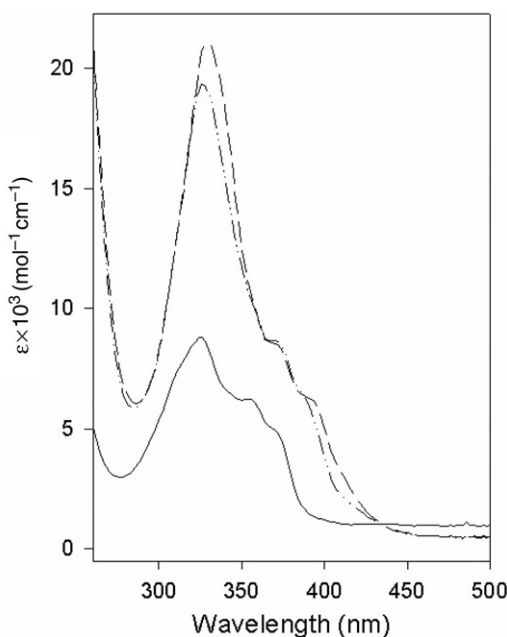
Figure 2. Electronic absorption spectra in the spectral range between 260 and 500 nm of Htrp (—), VO(trp)$_2$ (- - -), and VO(trp)$_2$Cl (—··—··).

Table 1. Electronic absorption spectra of free tropolone and the two oxovanadium complexes in DMSO solutions.

Tropolone		VO(trp)$_2$		VO(trp)$_2$Cl	
Band (nm)	ε (L mol^{-1} cm^{-1})	Band (nm)	ε (L mol^{-1} cm^{-1})	Band (nm)	ε (L mol^{-1} cm^{-1})
310 (sh)					
325	7.85×10^3	328	20.62×10^4	327	18.93×10^4
		338 (sh)		332 (sh)	
354 (sh)		372 (sh)		372 (sh)	
372 (sh)		394 (sh)		$\approx$388–390 (sh)	

attributed to the presence of two tropolone rings in the complexes and, eventually, by an additional enhancement of the main band by the contribution of a charge-transfer transition [33].

3.3. *Vibrational spectra*

3.3.1. Vibrational spectra of VO(trp)$_2$. The FTIR and FT-Raman spectra of VO(trp)$_2$, between 1700 and 400 cm^{-1}, are shown in figure 3; the proposed assignment is presented in table 2 and briefly discussed as follows:

– Assignment of the first two intense IR bands is based on arguments advanced by Junge [35] from an IR investigation of tropolone and its Cu(II) complex using
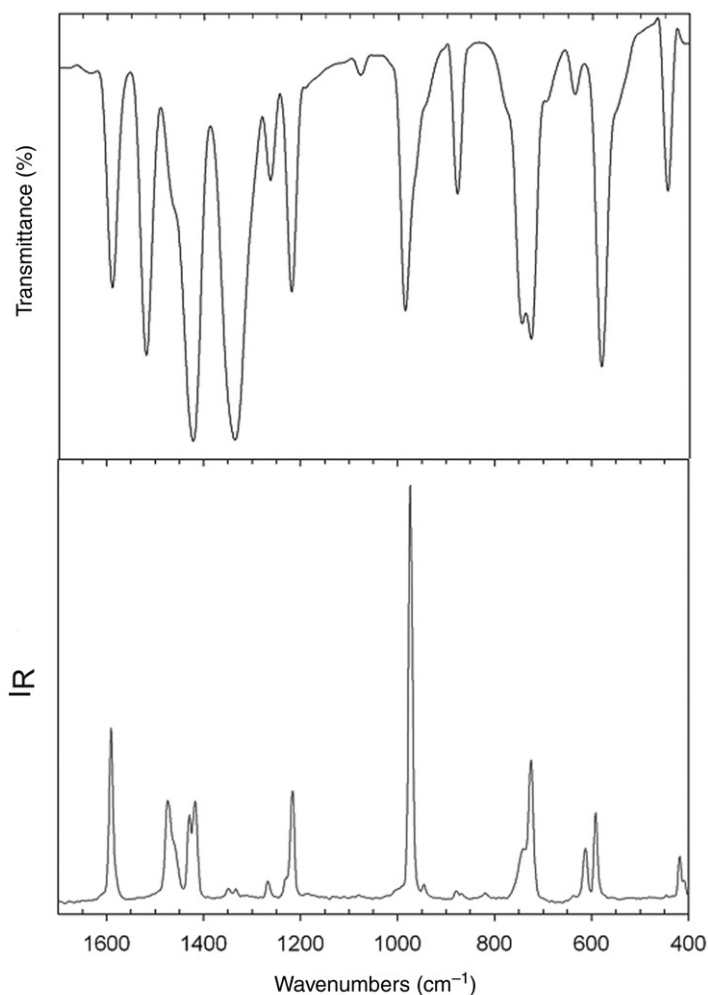
Figure 3. FTIR (above) and FT-Raman (below) spectra of VO(trp)$_2$ in the spectral range between 1700 and 400 cm^{-1}.

^{18}O-labeled tropolone. This study demonstrated that although ν(C=C) and ν(C=O) vibrations are strongly coupled, the higher energy band has more ν(C=C) character.

– In free tropolone, these bands are at 1608 and 1548 cm^{-1} in the IR and at 1607 and 1543 cm^{-1} in the Raman spectra. After complex formation both bands are displaced to lower energies and the second is absent in the Raman spectrum, or is eventually more strongly displaced up to 1474 cm^{-1}.

– There is another IR band at 1478 cm^{-1}, with Raman counterpart at 1460 cm^{-1}, in spectra of free tropolone which has some ν(C=O) character [35, 36]. This band is also displaced to lower energies in the complex and appears coupled to other vibrations (cf. table 2).

– The ν(C–OH) band is seen in free tropolone, partially coupled to ν(C–C) and δ(CH) vibrations, as a very strong IR doublet at 1268/1236 cm^{-1}, with Raman counterparts

Table 2. Assignment of FTIR and FT-Raman spectra of VO(trp)$_2$ from 1800 to 400 cm^{-1}.

IR (cm^{-1})	Raman (cm^{-1})	Assignment
1590 s	1591 s	ν(C=C) + ν(C=O)
1520 vs		ν(C=O) + ν(C=C)
1470 sh	1474 m	δ(CH)
1422 vs	1430/1420 m	ν(C=O) + ν(C–C) + δ(CH)
1336 vs	1357/1318 vw	ν(C=C)
1263 m	1272 vw	ν(C–C) + δ(CH)
1220 s	1217 s	ν(C–O)
1078 w		ν(C–C) + δ(CH)
986 s	973 vs	ν(V=O)
	950 vw	ν(C–C)
878 m	886/829 vw	ν(C–C) + δ(CH)
746/726 vs	740sh, 725 s	δ(CH) + ν(VO) (?)
690 sh		ν(C–C)
636 w	613 m	ν(VO)
581 vs, 550 sh	592 s	ν(VO)
445 m	418 w	ν(VO)

vs: very strong; s: strong; m: medium; w: weak; vw: very weak; sh: shoulder.

at 1272 and 1237 cm^{-1}. The corresponding δ(OH) vibration was identified as a medium intensity IR band at 1310 cm^{-1} and is absent in the Raman spectrum.

– In VO(trp)$_2$ the ν(C–O) of the now deprotonated OH-group is also displaced to lower frequencies in both the IR and Raman spectra and the δ(OH) mode is, obviously, absent.

– The strongest Raman line (973 cm^{-1}) is assigned to the characteristic V=O stretching vibration of the oxo group. Its IR counterpart lies at somewhat higher energy. This vibration lies in the usually expected range [37] but somewhat higher than in oxovanadium(IV) carbohydrate complexes [38, 39], in which the cation also has a similar VO$_4$ planar coordination as in the present complex. On the other hand, the position of this band clearly excludes the formation of bridging chain structures of the type $\cdots$V=O$\cdots$V=O$\cdots$V=O$\cdots$, for which much lower frequencies are expected [40].

– Some typical ring vibrations were also assigned on the basis of previous studies of other metal tropolonates [36, 41].

– In the low-frequency region, spectra of VO(trp)$_2$ have some new bands that are absent in spectra of the free ligand. Therefore, and also taking into account previous results [35, 36, 41], these bands are assigned to vibrations involving V–O (metal-to-ligand) bonds. Although in table 2 all these bands were identified as ν(VO), it is probable that some of them are originated in the deformational modes of the O=VO$_4$ skeleton.

3.3.2. Vibrational spectra of Co(trp)$_2$, Cu(trp)$_2$, and Zn(trp)$_2$. For comparative purposes, we have also measured and assigned vibrational spectra of Co(trp)$_2$, Cu(trp)$_2$, and Zn(trp)$_2$. Although IR spectra were reported earlier [40] the corresponding Raman spectra are reported here for the first time. The results of these measurements are presented in table 3. As it can be seen, the spectral patterns of these complexes resemble closely to that of VO(trp)$_2$.

Table 3.   Assignment of FTIR and FT-Raman spectra of Co(trp)$_2$, Cu(trp)$_2$, and Zn(trp)$_2$ from 1800 to 400 cm^{-1}.

Co(trp)$_2$		Cu(trp)$_2$		Zn(trp)$_2$		
IR	Raman	IR	Raman	IR	Raman	Assignment
1593 vs	1598 m	1590 s	1599s	1596 s	1598 s	ν(C=C) + ν(C=O)
1511 vs	1522 s	1515 vs	1510 w	1515 vs	1527 s	ν(C=O) + ν(C=C)
1471 vw	1492 vs	1470 sh	1472 vs	1473 vw	1474 vs	δ(CH)
1430 sh		1430 sh	1446 s	1435 m	1435 s	ν(C=O) + ν(C–C) + δ(CH)
1414 vs	1415 s	1412 vs	1410 vs	1412 vs	1420 m	ν(C=O) + ν(C–C) + δ(CH)
		1369 m	1369 m		1389 s	
1337 vs	1330 m	1343 vs	1333 m	1337 vs	1333m	ν(C=C)
1248 s	1248 s	1252 m	1228 m	1252 s	1253 s	ν(C–C) + δ(CH)
		1242 m	1242 m			δ(CH)
1220 vs	1225 m	1231 s	1231 s	1224 vs	1230 s	ν(C–O)
		1220 m				δ(CH)
1073 m		1075 w		1075 w		ν(C–C) + δ(CH)
996 m		998 w		1004 w		ν(C–C) + δ(CH)
972 m	975 s	970 w	973 s	974 w	976 s	ν(C–C)
915 m		918 m		917 m		ν(C–C)
874 s	879 m	874 s	875 w	876 s	875 m	ν(C–C) + δ(CH)
758 w		753 w		765 m		ν(C–C) + δ(CH)
744 w						δ(CH) + ν(MO)
726 vs		732 vs		734 vs		δ(CH) + ν(MO)
698 m	706 vs	711 m	711 s	697 m	708 vs	ν(C–C)
595 m	586 m	635 m	606 m	582 w	586 m	ν(MO)
529 s	536 m	586 vs	582 s	532 m	538 m	ν(MO)
420 m	428 m	423 s	417 s	425 m	429 s	ν(MO)

vs: very strong; s: strong; m: medium; w: weak; vw: very weak; sh: shoulder.

One interesting aspect of the Raman spectra is that the counterpart of the second very strong IR band, which is absent in the case of VO(trp)$_2$, can be clearly seen in Co(trp)$_2$ and Zn(trp)$_2$ whereas for Cu(trp)$_2$ it is present only as a very weak band.

A qualitative analysis of the last three Raman vibrations measured and assigned as ν(MO) vibrations in tables 2 and 3 shows that the first two increase in the order Co $\approx$ Zn < Cu < VO, whereas the third one does not show such a definite tendency. Besides, the Raman band at about 725 cm^{-1}, which is of complex origin but probably involves a MO vibrational mode, does not show a definite mass-depending trend.

3.3.3. Vibrational spectra of VO(trp)$_2$Cl. FTIR and FT-Raman spectra of this complex also show spectral patterns which are similar to those discussed above. The proposed spectral assignment is presented in table 4 and briefly commented as follows:

– In this case the higher energy band assigned to ν(C=C) + ν(C=O) is seen as a Raman doublet. Moreover, the second of these bands with the same origin, absent in the case of VO(trp)$_2$, is now present in the Raman spectrum as a medium intensity line at 1515 cm^{-1}.

– The 1283 cm^{-1} band is the strongest one in the Raman spectrum whereas its IR counterpart is seen as a medium intensity doublet.

– The characteristic ν(V=O) stretching is stronger in the IR spectrum, in which it also has a weak shoulder on the lower energy side, than in the Raman spectrum in which it appears somewhat broadened. The energy of this band is somewhat lower than that

Table 4. Assignment of FTIR and FT-Raman spectra of VO(trp)$_2$Cl (1800–400 cm^{-1}).

IR (cm^{-1})	Raman (cm^{-1})	Assignment
1588 s	1586 w/1571 s	ν(C=C) + ν(C=O)
1522 vs	1515 m	ν(C=O) + ν(C=C)
1460 w	1472 s	δ(CH)
1424 vs	1414 s	ν(C=O) + ν(C–C) + δ(CH)
1349 vs/1325 w	1352 m/1330 vw	ν(C=C)
1282 m/1263 m	1283 vs	ν(C–C) + δ(CH)
1214 m	1209 vs	ν(C–O)
1067 w	1064 w	ν(C–C) + δ(CH)
965 vs/941 sh	968 s	ν(V=O)
877 m	876 w	ν(C–C) + δ(CH)
766 sh/731 vs	734 s	δ(CH) + ν(VO) (?)
619 m	619 s	ν(VO)
580 vs	578 s	ν(VO)
543 m	542 s	ν(VO)
497 w, 472 w	498 vw	(?)
445 s/437 s	449 s/429 s	ν(VO)
416 m	402 vw	(?)

vs: very strong; s: strong; m: medium; w: weak; vw: very weak; sh: shoulder.

found in the VO(trp)$_2$ complex, a consequence of the presence of Cl$^-$ in the axial position, *trans* to the oxo group, which produces a weakening of the V=O bond.
– It is not easy to determine the position of the V–Cl vibration, although such bands related to terminal metal-chloride bonds are usually expected in the spectral range between 200 and 400 cm^{-1} [42]. On the basis of comparison of the IR and Raman spectra of the investigated complexes, we have tentatively assigned this vibration to a medium intensity Raman band at 359 cm^{-1}.

3.4. *Magnetic susceptibility of VO(trp)$_2$*

The temperature dependence of the molar paramagnetic susceptibility (χ_p) of the complex is shown in figure 4 and χ_p has a value of $1.493(3) \times 10^{-3}$ emu mol^{-1} at 298.5 K with corresponding effective magnetic moment ($\mu_{\text{eff}} = \sqrt{8\chi_p T}$) found to be $1.89\,\mu_B$, which is slightly higher than the μ_{eff}-value expected for magnetically diluted VO^{2+} (d^1) cations, that is, the spin-only value $1.73\,\mu_B$ or even less, if the orbital contribution is not completely quenched. On the other hand, effective magnetic moments larger than the spin-only value have been found for some oxovanadium(IV) complexes and explained from ferromagnetic interactions between vanadyl units through the formation of $\cdots$V=O$\cdots$V=O$\cdots$V$\cdots$ chains [43]. However, this latter possibility can be discarded for VO(trp)$_2$ taking into account the vibrational-spectroscopic behavior and analysis of the temperature dependence of the reciprocal molar paramagnetic susceptibility (χ_p^{-1}) (figure 5). The plot of χ_p^{-1} *versus* temperature follows a Curie law from 2 K up to about 50 K, but above this temperature there is a pronounced curvature which becomes more noticeable as the temperature increases. Taking into account the coordination geometry assumed for the complex, a distorted square pyramid with symmetry C$_{2v}$, the magnetic behavior may be explained considering a temperature-dependent susceptibility plus a temperature-independent paramagnetism (TIP), because such a coordination geometry,
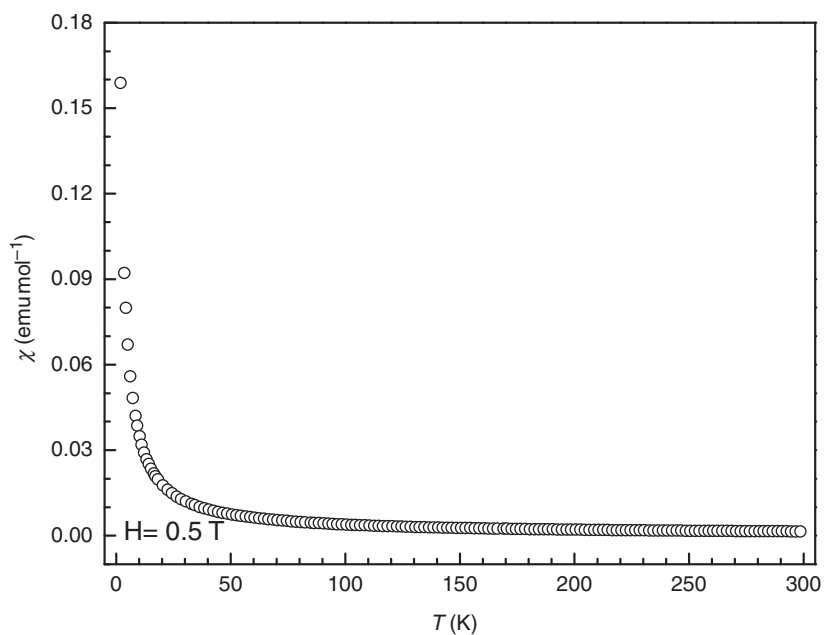
B.S. Parajón-Costa et al.

Figure 4.   Temperature dependence of the molar paramagnetic susceptibility (χ_P) of VO(trp)$_2$.
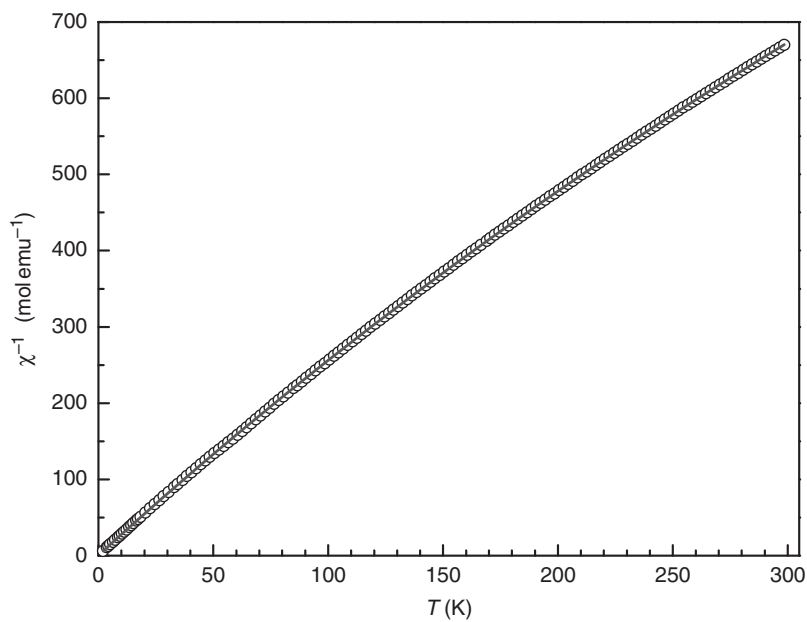

Figure 5.   Temperature dependence of the reciprocal molar paramagnetic susceptibility (χ_p^{-1}) of VO(trp)$_2$.

intermediate between the square pyramid (symmetry C_{4v}) and the trigonal bipyramid (symmetry D_{3h}), involves an orbitally non-degenerate ground state $^2A_2$ (d_{xy}) and the well above k_BT excited states $^2B_1$ (d_{xz}), $^2B_2$ (d_{yz}), $^2A_1$ ($d_{x^2-y^2}$), and $^2A_1$ (d_{z^2}) [44, 45]. Therefore, χ_p^{-1} data were fitted according to the equation $\chi_p = \frac{C}{T} + \chi_{TIP}$ (figure 5), yielding values of $C = 0.3624(2)$ emu K mol^{-1} and $\chi_{TIP} = 2.787(7) \times 10^{-4}$ emu mol^{-1}. The effective magnetic moment calculated from C ($\mu_{eff} = \sqrt{8\chi_{Curie}T} = \sqrt{8C}$) is 1.70 μ_B, which is in excellent agreement with the value of 1.71 μ_B calculated *via* $\mu_{eff} = g\sqrt{S(S+1)} = \frac{1}{2}g\sqrt{3}$ from the average g factor 1.972(5) determined previously from EPR measurements [32]. The χ_{TIP} term originates from the second-order Zeeman effect between the ground state and the excited states, and its value is inversely proportional to the energy differences between the $^2A_2$ (d_{xy}) ground state and the excited states, mainly $^2B_1$ (d_{xz}) and $^2B_2$ (d_{yz}). The obtained χ_{TIP} value is rather large compared with those of spin-single states in vanadium oxides, but is similar to those of the spin-singlet states of other VO^{2+} complexes [46].

3.5. *Electrochemical behavior*

The cyclic voltammogram of free tropolone, shown in figure 6 at $v = 0.1\,V\,s^{-1}$, displays one irreversible reduction peak (I) at $-1.54\,V$, which does not show any associated oxidation process in the reverse scan, even at the highest scan rate. The linear dependence of the cathodic peak potential Epc with log$v$ confirms the irreversibility of this peak [47]. On the reverse scan one small wave which shows anomalous behavior is observed at *ca* $-0.27\,V$. The dependence of this wave on electrode pretreatment suggests
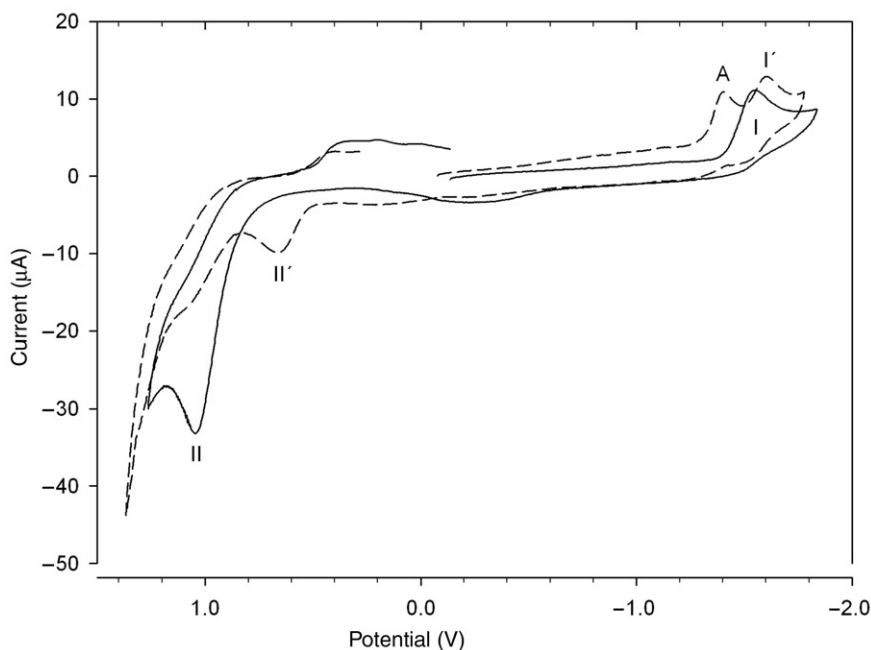

Figure 6. Comparative cyclic voltammograms of Htrp (—) and of VO(trp)$_2$ (- - - -) at $v = 0.1\,V\,s^{-1}$.

the adsorption of the reduction product on the electrode surface. Furthermore, at positive potential one oxidation peak (II) is observed at $+1.04$ V irrespective of the initial scan direction. A small reduction wave related to it appears on the reverse scan.

Due to the behavior of VO(trp)$_2$ solutions, section 3.2, the complex solutions employed in the electrochemical measurements were prepared directly in the electro-chemical cell using deoxygenated DMSO and working under a continuous N$_2$-gas stream.

The redox behavior of VO(trp)$_2$, at $v = 0.1$ V s^{-1}, is illustrated in figure 6. Two reductions and one oxidation are observed in the potential range investigated. The first peak (A) at -1.40 V gives no reverse signal on the subsequent anodic scan and shifts toward more negative values as v increases. The second irreversible peak (I$'$) situated at -1.60 V lies at a similar potential to that obtained with free tropolone. The current associated with this process was measured from decaying baseline of peak A. The cathodic current ratio ipc(A)/ipc(I$'$) values are close to one, at all investigated scan rates, indicating that the same number of electrons are involved in both processes. Furthermore, the current peak of both reductions, ipc(A) and ipc(I$'$), increases with the square root of the scan rate, $v^{1/2}$, approaching a single straight-line plot in accord with diffusion control [47]. According to the experimental data, the first cathodic peak (A) can be assigned to the irreversible reduction of the metal center from V(IV) to V(III) and the second one (I$'$) to a reduction of the coordinated ligand. On the forward anodic scan, the oxidation peak (II$'$) at $+0.66$ V with the small shoulder around 1.05 V corresponds to oxidation processes centered on the coordinated ligand. As shown in figure 6, the current intensity of this peak is smaller than that obtained with peak II suggesting that the coordination of the ligand modifies the number of electrons involved in this process.

Comparative voltammograms at $v = 0.1$ V s^{-1} for freshly prepared deoxygenated solutions of VO(trp)$_2$Cl and VO(trp)$_2$ are shown in figure 7.
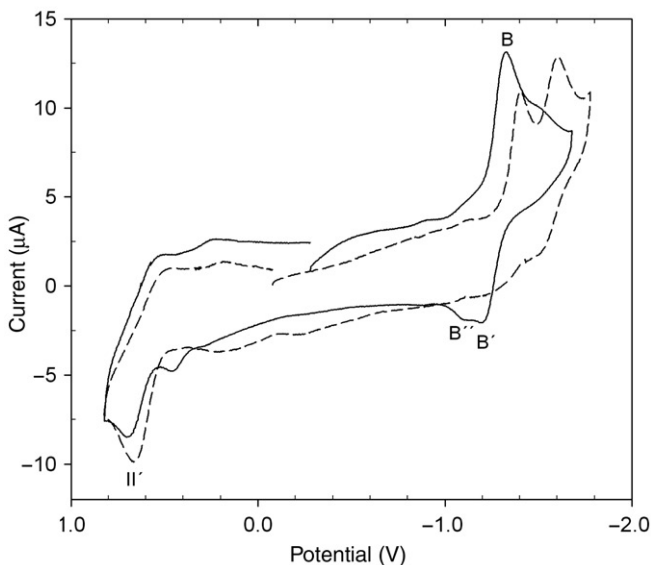
Figure 7.   Comparative cyclic voltammograms of VO(trp)$_2$ (- - - -) and VO(trp)$_2$Cl (—) at $v = 0.1$ V s^{-1}.

During the first cathodic cycle, the current/potential curve displays one reduction peak (B) at -1.30 V. On the subsequent anodic half cycle two oxidation signals (B′, B″) related to it appear at -1.20 and -1.10 V, respectively. The redox behavior of these peaks indicates that the cathodic process involves two sequential one-electron reductions of the metal center, V(V)/V(IV) and V(IV)/V(III), at very close potential values (EE mechanism) [47]. The two anodic peaks, on the reverse scan, correspond to the respective independent one-electron oxidations. The cathodic peak associated with reduction of the ligand is not clearly observed in the potential range investigated. Notwithstanding, the small wave between 1.40 and 1.65 V could correspond to this process. Anodic peak (II′) observed at $+0.70$ V for VO(trp)$_2$Cl lies at a similar potential and shows similar redox behavior to that obtained with VO(trp)$_2$ solutions. Thus, this process can be attributed to the oxidation of the coordinated ligand, as discussed above.

Finally, it must be noted that at more positive potential (not shown in figure 7) another irreversible process was observed at $+1.15$ V which could be attributed to the oxidation of chloride to elemental chlorine.

4. Conclusion

IR and Raman spectra of VO(trp)$_2$ and VO(trp)$_2$Cl are rather similar. Interestingly, the characteristic ν(V=O) stretching vibration lies at higher energy in the oxovanadium(IV) complex. The spectral patterns of these complexes are also very similar to those of bistropolonato complexes of Co(II), Cu(II), and Zn(II), investigated for comparative purposes. VO(trp)$_2$ solutions in different organic solvents are very unstable in air, rapidly oxidized. Voltamperommetric studies allowed determination of the potential at which V(IV)/V(III) reduction takes place in VO(trp)$_2$ and also showed that in VO(trp)$_2$Cl reduction of V(V) to V(IV) and V(III) involve two sequential one-electron processes at very close potential values. Magnetic susceptibility measurements of VO(trp)$_2$ were clearly compatible with the C$_{2v}$-symmetry assumed for this complex and showed that it has a relatively important TIP.

Acknowledgments

References

[1] K.H. Thompson, C.A. Barta, C. Orvig. *Chem. Soc. Rev.*, **35**, 545 (2006).
[2] K.H. Thompson, C. Orvig. *J. Inorg. Biochem.*, **100**, 1925 (2006).
[3] K.H. Thompson, J. Lichter, C. LeBel, M.C. Scaife, J.H. McNeil, C. Orvig. *J. Inorg. Biochem.*, **103**, 534 (2009).
[4] B.E. Bryant, W.C. Fernelius, B.E. Douglas. *Nature*, **170**, 247 (1952).

 [5] Y. Dutt, R.P. Singh, M. Katyal. *Talanta*, **18**, 1369 (1969).
 [6] E.L. Muetterties, H. Roesky, C.M. Wright. *J. Am. Chem. Soc.*, **88**, 4856 (1966).
 [7] T.J. Trust. *Antimicrob. Agents Chemother.*, **7**, 500 (1975).
 [8] Y. Morita, E. Matsumura, T. Okabe, M. Shibata, M. Sugiura, T. Ohe, H. Tsujibo, N. Ishida,
     Y. Inamori. *Biol. Pharm. Bull.*, **26**, 1487 (2003).
 [9] F.E. Jacobsen, J.A. Lewis, K.J. Heroux, S.M. Cohen. *Inorg. Chim. Acta*, **360**, 264 (2007).
[10] V. Kahn, A. Andrawis. *Phytochemistry*, **24**, 905 (1985).
[11] T.S. Chang. *Int. J. Mol. Sci.*, **10**, 2440 (2009).
[12] J.B. Helms, L. Huang, R. Price, B.P. Sullivan, B.A. Sullivan. *Inorg. Chem.*, **34**, 5335 (1995).
[13] M. Yamato, K. Ashigaki, N. Kokubu, T. Tashiro, T. Tsuruo. *J. Med. Chem.*, **29**, 1202 (1996).
[14] S.R. Budihas, I. Gorshkova, S. Gaidamakov, A. Wamiru, M.K. Bona, M.A. Parniak, R.J. Crouch,
     J.B. McMahon, J.A. Beutler, S.F.J. Le Grice. *Nucl. Acids Res.*, **33**, 1249 (2005).
[15] H. Shimanouchi, Y. Sasada. *Acta Crystallogr.*, **B29**, 81 (1973).
[16] B. Karlsson, A.M. Pilotti, A.C. Wiehager. *Acta Crystallogr.*, **B32**, 3118 (1976).
[17] J.E. Berg, B. Karlsson, A.M. Pilotti, A.C. Wiehager. *Acta Crystallogr.*, **B32**, 3121 (1976).
[18] J.E. Berg, A.M. Pilotti, A.C. Söderholm, B. Karlsson. *Acta Crystallogr.*, **B34**, 3071 (1978).
[19] M.C. Barret, M.F. Mahon, K.C. Molloy, J.W. Steed, P. Wright. *Inorg. Chem.*, **40**, 4384 (2001).
[20] E.J. Baran. *J. Inorg. Biochem.*, **80**, 1 (2000).
[21] E.G. Ferrer, A. Bosch, O. Yantorno, E.J. Baran. *Bioorg. Med. Chem.*, **16**, 3878 (2008).
[22] E.J. Baran. *Chem. Biodivers.*, **5**, 1475 (2008).
[23] G. Arrambide, D. Gambino, E.J. Baran. *J. Coord. Chem.*, **62**, 63 (2009).
[24] E.J. Baran. *J. Inorg. Biochem.*, **103**, 547 (2009).
[25] G. Arrambide, J. Rivadeneira, S.B. Etcheverry, B.S. Parajón-Costa, D. Gambino, E.J. Baran. *Biol. Trace Elem. Res.*, **132**, 176 (2009).
[26] C.M. Lee, C.S. Hwang. *J. Nano Biotechnol.*, **2**, 80 (2005).
[27] J.B. White, J. Selbin. *J. Inorg. Nucl. Chem.*, **32**, 2434 (1970).
[28] G.H. Rizvi, R.P. Singh. *Talanta*, **19**, 1198 (1972).
[29] G.A. Brain, J.F. Berry. *J. Chem. Ed.*, **85**, 532 (2008).
[30] H.M. Koepp, H. Went, H.Z. Strehlow. *Z. Elektrochem.*, **64**, 483 (1960).
[31] R.R. Gagné, C.A. Koval, G.C. Lisensky. *Inorg. Chem.*, **19**, 2854 (1980).
[32] C.P. Stewart, A.L. Porte. *J. Chem. Soc., Dalton Trans.*, 1661 (1972).
[33] M. Hasegawa, Y. Inomaki, T. Inayoshi, T. Hoshi, M. Kobayashi. *Inorg. Chim. Acta*, **257**, 259 (1997).
[34] L.C.T. Shoute, V.J. MacKenzie, K.J. Falk, H.K. Sinha, A. Warsylewicz, R.P. Steer. *Phys. Chem. Chem. Phys.*, **2**, 1 (2000).
[35] H. Junge. *Spectrochim. Acta*, **24A**, 1957 (1968).
[36] Y. Jianlin, Y. Yaxian, G. Renao. *Spectrochim. Acta*, **64A**, 1072 (2006).
[37] J. Selbin. *Chem. Rev.*, **65**, 153 (1965).
[38] E.J. Baran. *J. Coord. Chem.*, **54**, 215 (2001).
[39] E.J. Baran. *J. Inorg. Biochem.*, **103**, 547 (2009).
[40] M. Mathew, A.J. Carty, G.J. Palenik. *J. Am. Chem. Soc.*, **92**, 3197 (1970).
[41] L.G. Hulet, D.A. Thornton. *Spectrochim. Acta*, **27A**, 2089 (1971).
[42] K. Nakamoto. *Infrared and Raman Spectra of Inorganic and Coordination Compounds*, 5th Edn, John Wiley, New York (2009).
[43] R. Sáez-Puche, J. Romero, A.C. González-Baró, E.J. Baran. *Chem. Phys. Lett.*, **282**, 273 (1998).
[44] C.J. Ballhausen, H.B. Gray. *Inorg. Chem.*, **1**, 111 (1962).
[45] A.R. Rossi, R. Hoffmann. *Inorg. Chem.*, **14**, 365 (1975).
[46] J. Costa Pessoa, I. Tomaz, R.T. Henriques. *Inorg. Chim. Acta*, **356**, 121 (2003).
[47] A.J. Bard, L.R. Faulkner. *Electrochemical Methods: Fundamentals and Applications*, 2nd Edn, John Wiley, New York (2001).